Review

Polymer Bead Foams: A Review on Foam Preparation, Molding, and Inter-Bead Bonding Mechanism

Junjie Jiang , Liang Wang , Fangwei Tian , Yaozong Li , Wentao Zhai *

Posted Date: 7 September 2023

doi: 10.20944/preprints202309.0439.v1

Keywords: bead foams; molding method; inter-bead bonding; molding mechanism

Review

Polymer Bead Foams: A Review on Foam Preparation, Molding, and Inter-Bead Bonding Mechanism

Junjie Jiang [1,2], Liang Wang [1], Fangwei Tian [1,2], Yaozong Li [1,2] and Wentao Zhai [1,2,*]

[1] School of Materials Science and Engineering, Sun Yat-sen University, Guangzhou 510275, China
[2] Nanchang Research Institute Sun Yat-sen University, Nanchang 330224, China
* Correspondence: zhaiwt3@mail.sysu.edu.cn; Tel./Fax: +86-020-8411-3428

Abstract: The diverse physical appearances and wide density range of polymer bead foams offer immense potential across various applications and future advancements. The multi-scale and multi-level structural features of bead foams involve many fundamental scientific topics. This review presents a comprehensive overview of recent progress in bead foams preparation and molding techniques. Initially, a comparative analysis is conducted among bead foam characteristics of distinct polymers, based on their unique properties. Subsequently, a summary and comparison of molding processes employed for fabricating bead foam parts are provided. Beyond traditional methods like steam-chest molding (SCM) and adhesive-assisted molding (AAM), emerging techniques like in-mold foaming and molding (IMFM) and microwave selective sintering (MSS) are highlighted. Lastly, the bonding mechanisms behind the diverse molding methods are discussed.

Keywords: bead foams; molding method; inter-bead bonding; molding mechanism

1. Introduction

Physical foaming uses gases such as carbon dioxide (CO_2) or nitrogen (N_2) as foaming agents, providing the benefits of environmental friendliness and no residue of harmful substances [1,2]. As a result, the fabrication of polymer foams by physical foaming has received increasing attention. Polymer foams can be categorized into bead foams/foamed beads, foamed sheets, foamed boards, and foamed profiles based on product shapes [3,4]. Bead foams generally require molding into the final parts. The structural design of the mold allows to produce bead foam parts with complex shapes and rich appearance patterns [5,6]. New categories of bead foams have been continuously developed since the introduction of expandable polystyrene (EPS) around 1950. An increasing number of bead foam types have been developed to meet higher requirements, especially after 2000. Due to the advantages of low density and complex shapes, bead foam parts have found extensive applications in various fields, including cold chain logistics, goods packaging, sports protection, and automotive interiors.

Figure 1 illustrates the multiscale and multi-level structure of bead foams, ranging from nanometers to centimeters. Each scale is associated with various research topics. From the perspective of molecular chains, the variety of bead foam types has expanded from the initial PS [7,8] to polyethylene (PE) [9], polypropylene (PP) [10-13], thermoplastic polyurethane (TPU) [4,14-16], poly lactic acid (PLA) [17], and other polymers. Regulatory strategies for foaming behavior differ based on differences in the chains structure. For instance, the key to PP foaming primarily depends on the regulating crystalline structure and melt strength. The microcellular structure of foamed beads influences the moldability and the mechanical properties of the final products. Therefore, acquiring the desired cell morphology, such as cell size, cell density, and open cell content, is critical to the preparation of bead foams. Bead foams can be classified into two categories, one is the expandable particles represented by EPS, which contain volatile gases. The other type of bead foams is expanded/foamed beads, which are generally prepared by autoclave foaming. Autoclave foaming involves filling polymer pellets into an autoclave, which are then saturated with high-temperature

 doi:10.20944/preprints202309.0439.v1

and high-pressure gas. During saturation stage, the gas diffuses into the polymer and affects the condensed structure of the polymer chains. In general, water is used as a dispersion medium to ensure uniform heating of pellets and to prevent conglomeration. To improve production efficiency, anhydrous autoclave foaming has been developed and implemented in the production of expanded TPU (ETPU) beads. Furthermore, bead foams production can also be achieved through extrusion foaming, where the crucial factor is matching an appropriate granulation unit [11,18]. Bead foams prepared through extrusion foaming suffer from issues of low cell uniformity and a high open-celled content when compared to those produced through autoclave foaming [19,20]. Nonetheless, continuous process and high production stability have made extrusion foaming the most promising method for producing bead foams in the future.

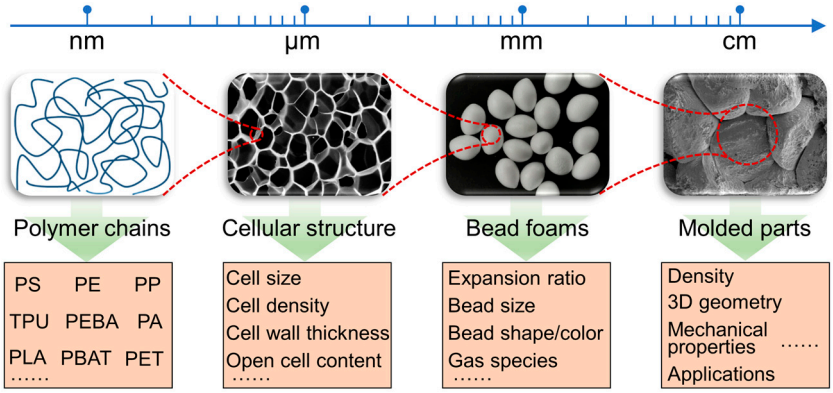

Figure 1. Multiscale and multi-level structures in bead foams and related research topics.

Bead foams are rarely used directly and need to be molded into bead foam parts to maximize their benefits. The evaluation of molding effect mainly considers appearance quality and bonding strength between beads, which directly affects the application of the molded parts [21]. Through the design of the mold surface, the parts can obtain a rich appearance pattern. Steam-chest molding (SCM) is one of the most important and widely utilized molding process for bead foams. During the SCM process, the foamed beads are injected into the mold while saturated steam is employed as the heating medium to soften the beads and induce inter-bead bonding. Achieving sufficient inter-bead bonding while maintaining a stable cell structure is crucial for the molding process. It has been suggested that the sintering of bead foams is closely related to their thermal properties. Inspired by SCM, various methods for molding bead foams have been developed, such as adhesive-assisted molding (AAM) [22-24], in-mold foaming and molding (IMFM) [6,25], microwave selective sintering (MSS) [26,27], etc. Nevertheless, the molding mechanisms behind these methods are seldom discussed and compared systematically.

This article presents a systematic overview of the recent research progress on bead foams, which covers essential aspects such as the methods of bead foams preparation and molding. In particular, the common issues involved in the bead foam molding process and the molding mechanism are discussed. This review could provide theoretical guidance for the development of new types of bead foams.

2. Preparation of bead foams

Typically, the fabrication of bead foam parts involves two steps: preparation of foamed beads/bead foams and molding these bead foams into final parts. As shown in Figure 2, the preparation method of bead foams mainly includes autoclave foaming and extrusion foaming. Autoclave foaming is a batch process, during which polymer pellets are saturated with high pressure gas under temperatures lower than their melting point, and foaming occurs upon rapid depressurization [4,28]. Extrusion foaming is a continuous process to prepare bead foams, which requires additional granulator system [11,12,20].

Preprints (www.preprints.org) | NOT PEER-REVIEWED | Posted: 7 September 2023 doi:10.20944/preprints202309.0439.v1

The properties of the polymer itself play a critical role in the production of bead foams. Crystallization properties, melt strength, and modification of molecular chains (such as grafting and blending), as well as interaction with saturated gases, have a significant impact on the foaming behavior. Therefore, different strategies are necessary for various polymers to achieve the desired properties in bead foams. The following sections will discuss the preparation of bead foams based on different polymers.

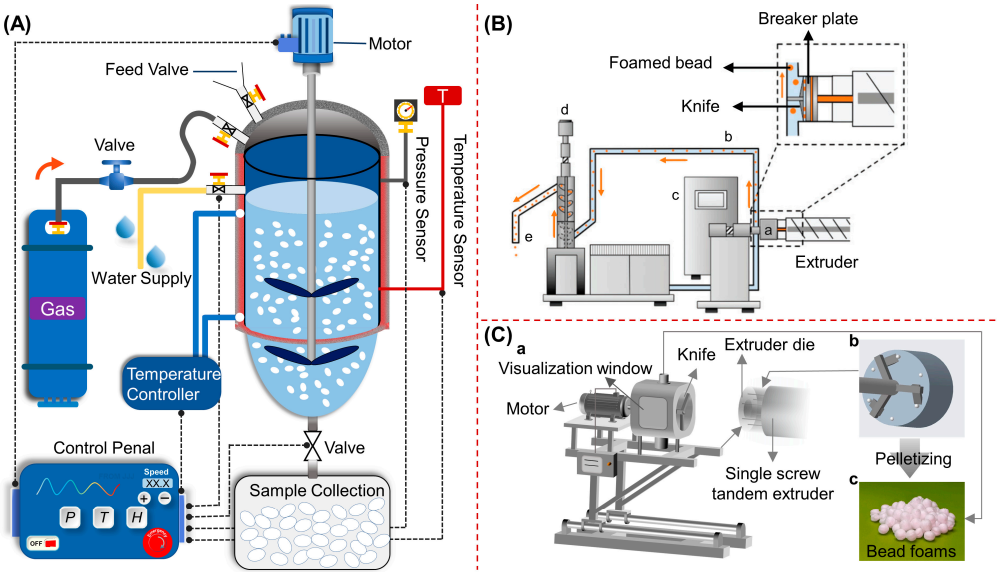

Figure 2. Schematic of autoclave foaming with water as the dispersion medium (A). Reproduced with permission from [1], Copyright 2021 Taylor & Francis Group. Extrusion foaming equipped with an underwater granulator (B). Reproduced with permission from [20]. Extrusion foaming equipped with a winder-cooling pelletizer (C). Reproduced with permission from [11]. Copyright 2022 American Chemical Society.

2.1. Expandable polystyrene (EPS) beads

EPS foams account for the largest share of the bead foam market. The development of EPS was begun in 1949, when chemist Fritz Stastny at BASF successfully produced the material in laboratory. Generally, blowing agent (usually pentane) was introduced in PS suspension polymerization process to produce EPS beads, which contain 4–7 wt% blowing agent. EPS beads are produced in the form of small grains. Usually, EPS beads could not be used alone, which needed to be pre-expanded and molded into final parts with various geometry [29]. Molded parts produced from EPS beads offer several advantages such as excellent thermal insulation, low density, low moisture absorption, and a relatively low cost. Additionally, EPS production process is simple. Due to these benefits, EPS parts are widely used in various applications such as packing, building insulation [8], transportation and flotation foams. However, the intrinsic flammable features of EPS prevent it from being directly used in specific fields such as building insulation [8,30,31]. Consequently, research on EPS has focused mainly on adding multi-functionality, particularly flame-retardant properties, to EPS using a variety of methods.

The incorporation of various fillers in the polymerization process has been demonstrated as an effective method for manufacturing multifunctional EPS beads. Recently, hydrophobic Fe_3O_4 was incorporated into EPS by means of in situ suspension polymerization of styrene (Figure 3) [7]. The authors systematically studied the effects of different experimental variables, such as Fe3O4 content, stirring speed, and the amount of surfactant, on the size and magnetic properties of the expandable PS/Fe_3O_4 beads. SEM and energy-dispersive spectrometer results showed that Fe_3O_4 was well dispersed in the synthesized colorized and magnetic beads. It was proposed that the bead size and size distribution, as well as the degree of color could be adjusted by altering the Fe3O4 content. Flame retardants – such as aluminum hydroxide, ammonium polyphosphate, magnesium hydroxide –

Preprints (www.preprints.org) | NOT PEER-REVIEWED | Posted: 7 September 2023 doi:10.20944/preprints202309.0439.v1

could be coated onto the surface of EPS beads or incorporated into PS chains via suspension polymerization. Hong et al. [32] used methylene diphenyl diisocyanate (MDI) as binding agent to improve the compatibility between intumescent flame retardant and EPS beads. cone calorimeter tests showed that the parts made by MDI-coated flame-retarded EPS exhibited good flame resistance performance. By incorporation the flame retardants into EPS through in situ polymerization, Bai et al. [31] prepared halogen-free flame-retardant EPS beads. The fire retardant, called hexaphenoxycyclotriphosphazene (HPCTP), was uniformly dispersed in the PS matrix at nanoscale. The particles formed by HPCTP were of the order of 33 − 57 nm and the average diameter was 44.86 nm. The mechanism of flame retardancy was also proposed based on the microscale combustion calorimetry results. In addition, fillers could be deposited on the surface of EPS beads. Lelis et al. [33] prepared SiO2 coated EPS beads by physical vapor deposition. The EPS beads were then pre-expanded and molded into EPS parts. The resulting expanded PS coated with SiO2 additives had almost 10% lower moisture adsorption and an 8.4% better deformation resistance. Surprisingly, the molded parts showed enhanced inter-bead bonding strength, which could be due to the SiO_2 acting as a binder.

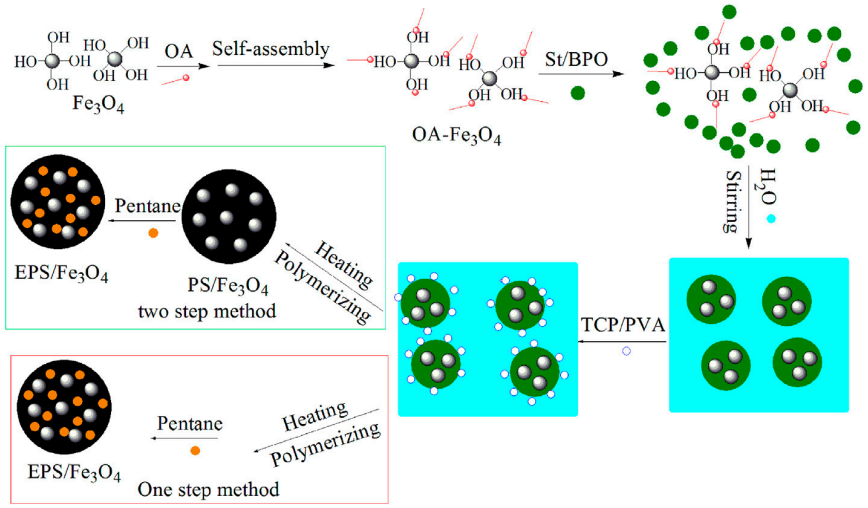

Figure 3. Schematic of the synthesis route of colorized PS/Fe3O4 beads and EPS/Fe3O4 beads. Reproduced with permission from [7].

2.2. Expanded polypropylene (EPP) beads

EPP have attracted much attention since its invention in the 1980s. EPP parts molded from the foamed beads show excellent solvent resistance, high impact resistance, and good heat resistance, high energy absorption capacity. EPP beads are typically fabricated by autoclave foaming. The foaming temperature window for EPP beads is very narrow due to the high crystallinity and low melt strength. The destruction of PP crystals during autoclave foaming results in a significant reduction in the melt strength, making it challenging to prepare EPP beads with desired properties [34]. Therefore, copolymerization with α-olefin or molecular modification to improve the foaming behavior and reduce the processing difficulty are necessary [13,35,36]. Furthermore, the crystalline structures of PP are sensitive to foaming conditions, such as temperature profile, gas type and pressure, and saturation time. As a result, the foaming process should be carefully adjusted to achieve the expected foaming results.

Park et al. [37] studied the foaming behavior of EPP beads using CO_2 as the blowing agent in a lab-scale autoclave and systematically discussed the critical processing variables for EPP beads production. It was found that an optimum stirring speed, which dependent on the shape of stirring propeller and channel sizes, was necessary to allow a uniform distribution of PP pellets in the dispersing media. Meanwhile, it was proposed that die geometry and saturation pressure are the key to pore morphology and thermal properties of EPP beads. When the pressure increased from 3.8 to 5.5 MPa, the cell density increased nearly one order of magnitude and the expansion ratio increased

 doi:10.20944/preprints202309.0439.v1

from 3.4 to 16.4 times. In another study conducted by the same group, Nofar et al. [38] explored the effect of various foaming parameters on the formation of double melting peak in EPP beads with the help of a high-pressure DSC. It was demonstrated that the thermal properties of PP samples were strongly affected by the saturation temperature and pressure. An increase in saturation temperature in an appropriate range facilitated the crystals perfection to form a higher melting peak ($T_{m\text{-}high}$). Meanwhile, the melted crystals formed a lower melting peak ($T_{m\text{-}low}$) during the cooling stage. Similarly, Guo et al. [39] also demonstrated that the double melting peak temperature in EPP beads shifted to higher value with an increase in saturation temperature and pressure. The formation of double melting peak in EPP beads is helpful to the sintering of foamed beads.

To improve the foamability of linear PP, several methods for increasing expansion ratio or optimizing cellular structure have been employed, including copolymerization, blending and modification (like grafting, cross-linking). The type and content of comonomer in PP copolymers have a significant influence on the foaming behavior of EPP beads [34]. Park et al. [34] used a pilot autoclave to compare the difference in the foaming behavior of a linear PP and PP copolymers containing ethylene comonomer. They reported that the addition of 3.5 wt% ethylene comonomer reduced the crystallinity and melting temperature (T_m) of PP resin, improving the PP foamability and increasing the cell size. By blending 3 – 8 wt% high melting point PP, Hu et al. [40] found that the cellular morphology and melting properties of EPP beads based on low melting point PP could be improved. Guo et al. [36] fabricated high melt strength polypropylene (HMSPP) by direct polymerization and discussed the impact of melt strength on the cellular morphology and properties of EPP beads obtained by autoclave foaming. They found that EPP beads prepared from HMSPP had more uniform and well-distributed cells than that from polypropylene homopolymer. Janani et al. [41] investigated the role of polymorphism in the production of EPP bead foams with double melting point and concluded that the utilization of polymorphism during solid-state foaming is a feasible way to prepare EPP beads with nano-sized cells.

Reducing the energy consumption is one trend in the preparation of bead foams. Strategies such as blending PP with various polyolefin components or copolymerization propylene with other short-chain alkene have been utilized to fabricate EPP beads with moderate foaming conditions. Lyu et al. [13] synthesized various ethylene−propylene−butene-1 ternary copolymer (TPP) and ethylene−propylene copolymer and investigated the autoclave foaming behavior of these copolymers. It was found that the addition of 1-butene could reduce 5 °C for TPP in saturation temperature when the expansion ratio of EPP beads was identical. Huang et al. [42] found that the temperature and pressure could be reduced by blending a certain amount of polyputene-1 (PB-1) during the autoclave foaming of EPP beads without compromising the expansion ratio. Additionally, n-pentane has a significant plasticization effect on PP. Compared with CO_2 as the blowing agent, Zhai et al. [43] have reported that using n-pentane as the foaming agent during PP autoclave foaming could result in an obvious reduction in the foaming temperatures from 150 − 153 °C to 92 − 96 °C, an increase in the expansion from 8 − 20 to 10 − 50 fold, and an increase in the cell density from $10^5 - 10^8$ to $10^7 - 10^9$ cells/cm^3. Lower foaming temperatures and higher expansion ratios reduce the production energy consumption, which enhances the competitiveness of EPP foams.

Although there was much research focused on the extrusion foaming of PP, these studies mainly investigated the preparation of foamed strands not foamed beads [18,35,44-47]. Recently, Huang et al. [12] successfully manufactured EPP beads by a commercially available extrusion line equipped with the self-designed wind cutting tool. They studied the cell growth behavior after the foam exited the extruder die using a high-definition camera. As shown in Figure 4, EPP beads with various shapes and sizes could be easily produced by adjusting the pelletizing speeds. The obtained foamed beads had a lowest density of 0.052 g/cm^3 and the open cell content of the beads were higher than 50%. In another work on extrusion foaming, Huang et al. [11] improved the cell uniformity of EPP bead by blending 10 wt% TPU resin. A more uniform cell morphology contributes to a better mechanical strength of EPP molded parts. With the help of a foam extrusion line designed by Sulzer, Tammaro et al. [10] produced EPP beads with the bulk density ranging from 20 to 100 g/cm^3. They used a long chain branched HMSPP as the feedstock and CO_2 and isobutane as the blowing agent. It was

Preprints (www.preprints.org) | NOT PEER-REVIEWED | Posted: 7 September 2023 doi:10.20944/preprints202309.0439.v1

proposed that strain hardening feature of HMSPP made it easier to produce EPP beads with lower open cell content.

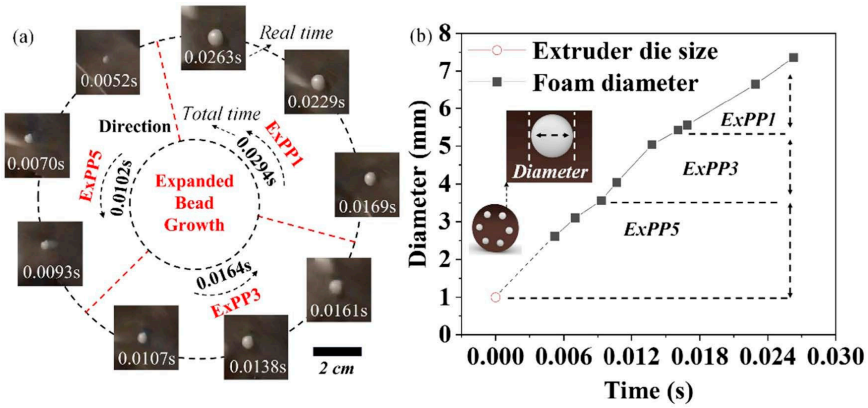

Figure 4. (a) Using high-definition camera (set at 3840 frames/s (x128 times)) to record the real-time cell growth of the beads at different pelletizing speeds, and (b) the diameter size curve of the bead foams (before leaving the extruder die) as a function of time. Reproduced with permission from [12]. Copyright 2022 Elsevier.

EPP beads produced through autoclave foaming usually display closed and uniform cell structures; however, the beads prepared by the extrusion foaming process exhibit a higher content of open cells and less uniformity. How to achieve high uniform and closed cells in the extrusion foaming process is an important problem need to be solved.

2.3. Expanded thermoplastic polyurethane (ETPU) beads

TPU is a category of TPE, which is composed of soft segments and hard segments. Oligomer diols with low glass transition temperature (T_g) such as poly(tetramethylene glycol) [48] acted as soft segments, which endow TPU with excellent stretchability and elasticity. ETPU beads with pore structures exhibit many advantageous properties including low density, high resilience, and cushioning effect [15,16]. A lot of research efforts has focused on elucidating the relationship between the TPU molecular chains' structure and foaming behavior, strategies for suppression of the shrinkage of the foamed beads, and the adjustment of the foaming process [49-51].

The foaming behavior of ETPU beads is affected by the chemical structure, composition ratio, and molecular weight of the hard and soft segments in TPU. Nofar et al. [52] investigated the effects of hard segments content on the foaming behaviors of TPU pellets. The hard segment content in the TPU resins were 39 wt%, 49 wt%, and 57 wt%, and the corresponding Shore hardness of these pellets were 29D, 46D and 64D, respectively. Ordered structures with higher perfection formed in TPU with higher hard segments content, thus leading to higher melting temperatures. An increase in the hardness broadened the foaming temperature window and increased the suitable foaming temperature. For TPU with the highest hardness, 64D TPU exhibited lowest shrinkage ratio, but the expansion ratios of foamed samples were lower than 3-times. Furthermore, they compared the foaming behavior of TPUs with similar hard segments but different type of soft segments (polyester and polyether type) [53]. Compared with polyether based TPU, polyester based TPU showed a wider foaming temperature window. When the temperature increased from 85 °C to 115 °C, the polyether based TPU formed a larger and more closed packed microcrystalline under supercritical CO_2 conditions, which might hinder the growth of the nucleated cells and led to a limited expansion ratio of the foamed beads. Additionally, the effects of thermal annealing and pressure drop rate on foaming behavior were also explored. In their another study, Nofar et al. [54] had further studied the impact of different soft segments molecular weight on the foaming performance of TPU pellets. TPU with three soft segment molecular weights of 1000 g/mol, 2000 g/mol and 3500 g/mol were selected. It was found that an increase in soft segment molecular weight reduced the T_g of the soft segments, promoted the formation of wide ordered hard segments accumulation and led to a broader melting

Preprints (www.preprints.org) | NOT PEER-REVIEWED | Posted: 7 September 2023 doi:10.20944/preprints202309.0439.v1

range and wider foaming temperature window. It was also observed that increasing the length of soft segments could not only facilitate the expansion of the bead foams, but also enhance the crystallization of hard segments, thereby promoting heterogeneous cell nucleation and reducing the shrinkage of the foamed samples (Figure 5).

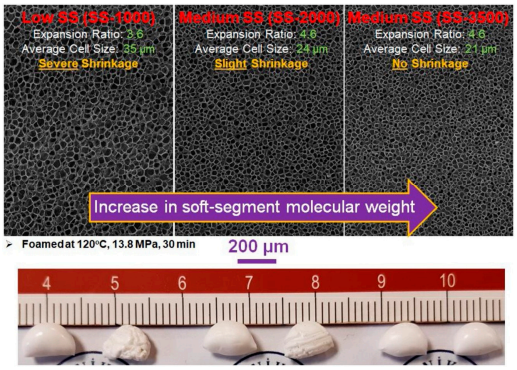

Figure 5. Evolution of the cellular morphology of ETPU beads with the increase in soft segments molecular weight. Reproduced with permission from [54]. Copyright 2020 Elsevier.

Based on the theory that hard domains could act as heterogeneous nucleating agent, it was argued that the adjustment of cellular morphology of TPE foams could be realized by changing the degree of ordering of hard segments [55-58]. Park et al. found that large amount of less ordered hard segments micro-crystallites in TPU induced by glycerol monosterate and high-pressure butane could promote cell nucleation and thus increase the cell density [56]. A similar result was also observed by the same group in PEBA foams [57].

The formation of cellular structures in polymer requires enhanced molecular mobility at elevated temperature. Jiang et al. [4] defined the "high-elastic state" of TPU by softening temperature (T_s) and viscous flow temperature (T_v) and associated the molecular movement with the autoclave foaming behavior of TPU pellets. In the "high-elastic state", the polymer chain motion was significantly enhanced, and large deformation of the entire molecular chain was possible. Within this state, the low-ordered hard segments disassociated and mixed into the soft segment domains, while part of the hard segments rearranged into more closed packed. The hard segments of different order acted as nucleation sites to promote cell nucleation, and the nucleated cell could expand to a large extent under the "high elastic state". The soft segment chains were significantly stretched, and some of the hard segments dissociated and rearranged, eventually leading to the formation of cell structures. ETPU beads with high expansion ratio were obtained within the temperature range defined by the "high elastic state" (Figure 6). Another study conducted by Jiang et al. [55] demonstrated that the proposed "high elastic state" could also be used to explain the autoclave foaming behavior of EPEBA beads.

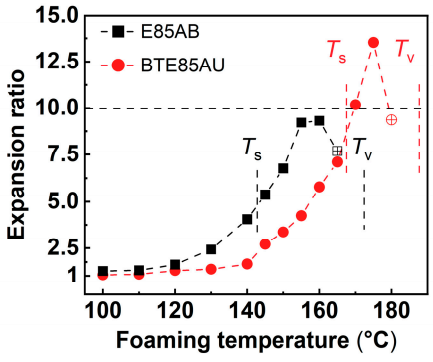

Preprints (www.preprints.org) | NOT PEER-REVIEWED | Posted: 7 September 2023 doi:10.20944/preprints202309.0439.v1

Figure 6. Expansion ratios of ETPU beads as a function of foaming temperature. Hollow dots indicate the occurrence of fusion bonding between the ETPU beads. Reproduced with permission from [4]. Copyright 2021 Elsevier.

Post-foaming shrinkage is a common phenomenon in TPE physical foaming, and the shrinkage mechanism has been widely discussed [1,59,60]. On one hand, the rate of gas diffusion out of the cells is much faster than the rate of the air diffusion into the cells, creating a negative pressure in the pores. On the other hand, the cell walls of TPE foams have a low modulus and cannot resist the compressive force generated by negative pressure. Figure 7 shows the shrinkage behavior of ETPU beads obtained over a wide range of foaming temperatures. After foaming, the expansion ratios of the ETPU beads were very high, even higher than 25 times. However, these foamed beads shrunk seriously with the gas diffusion out of the cells. When the air fully diffuses into the cells, the shrunk beads will "expand" again to a certain degree. To reduce the shrinkage ratio of TPE foams, strategies such as blending with plastics [61,62], chemical cross-linking [63,64], using gas mixture as blowing agent [49,65], compounding with fillers [66,67] have been proposed. Detailed discussion could be found in the review on physical foaming of TPE [1].

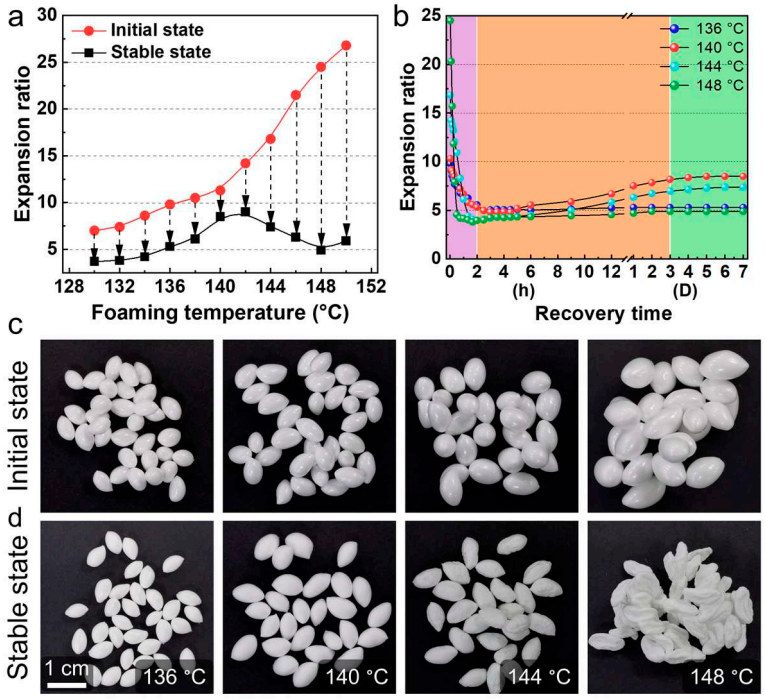

Figure 7. Comparation of the expansion ratio of TPU foamed beads in the initial and stable state (a), evolution of the expansion ratio of TPU foamed beads after foaming (b), digital photos of TPU foamed beads in the initial and stable state (c-d). Reproduced with permission from [25]. Copyright 2023 Elsevier.

2.4. Expanded polylactic acid (EPLA) beads

PLA is a biodegradable plastic synthesized from biological resources, which is widely used in food packaging and biomedicine due to its good biodegradability and biocompatibility. At the same time, PLA is also considered an ideal alternative to petroleum-based plastics to address the growing problem of plastic pollution. A great deal of research is devoted to the production of PLA foams by physical foaming. The introduction of cellular structure can make PLA lightweight without affecting the biocompatibility of PLA and accelerate the degradation rate of PLA foams [68].

EPLA beads are mainly produced by autoclave foaming technology. During autoclave foaming process, crystal structure [69], molecular weight [70] and molecular architecture play a vital role in the foaming behavior of EPLA beads [71]. PLA has the problem of low melt strength, which makes it difficult to foam. Chemical modification has been proven to be effective to improve the foamability

Preprints (www.preprints.org) | NOT PEER-REVIEWED | Posted: 7 September 2023 doi:10.20944/preprints202309.0439.v1

of PLA. Altstädt et al. [70] incorporated various chemical modifiers into PLA by reactive extrusion using a twin-screw extruder. It was found that the modified PLA exhibited higher molecular weight and reduced crystallinity. The incorporation of organic peroxide and multifunctional epoxide resulted in the most significant increase in the molecular weight and polydispersity of PLA. Under the foaming conditions of 157 °C/0.5 h/18 MPa, all the modified PLA foams showed a reduced density, with a low density of 107 kg/cm^3. An increase in extensional viscosity of modified PLA also led to larger cells because the cells had more time to expand before cell coalescence. Using a long chain branched PLA, Park et al. [69] investigate the formation of double melting peaks in PLA bead foams. They found that high pressure CO_2 saturation would dramatically affect the crystal structure of PLA, thus altering the cellular morphology of PLA foams. On the one hand, during the high pressure CO_2 saturation process, the formation of a small number of perfected crystals of large size would increase the high melting temperature. On the other hand, the foaming and cooling steps would destroy part of the crystals and induce the formation of the low melting peak.

As a biopolymer, PLA is highly susceptible to hydrolytic degradation, especially under the high pressure CO_2 saturation process during autoclave foaming. Under the saturation of 120 °C/5.5 MPa/ 15 min, Park et al. found that the Mw decreased from 360 kg/mol for raw pellets to about 305 kg/mol for EPLA beads [72]. When the saturation temperature was gradually increased to 126 °C, more hydrolysis occurred, and the M_w of the foamed sample was slowly reduced to about 285 kg/mol (Figure 8). The hydrolysis of PLA is very sensitive to the saturation time. Under the saturation of 120 °C/5.5 MPa, it was observed that the M_w was dramatically reduced from 300 kg/mol to 160 kg/mol when the saturation time was extended from 15 min to 60 min. These results suggest that the saturation condition should be properly selected to control the extent of hydrolysis to produce EPLA beads with desirable cellular morphology and expansion ratio. By compounding PLA with a hydrolysis stabilizer via reactive extrusion, Bonten et al. [28] found that the hydrolysis of PLA during autoclave foaming could be markedly suppressed without compromising the foamability of EPLA beads.

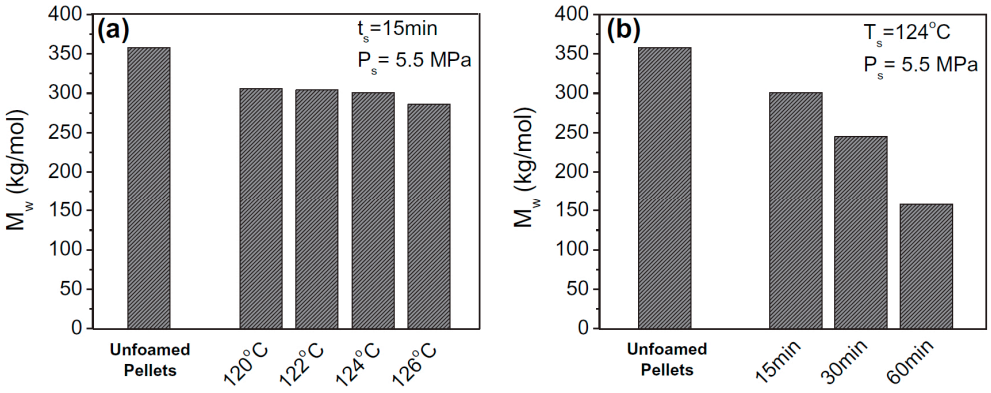

Figure 8. The average molecular weight of the EPLA beads saturated at different temperatures (a) and times (b). Reproduced with permission from [72]. Copyright 2015 Elsevier.

2.5. Bead foams based on other polymers

Although bead foams of the aforementioned polymer types are prevented in the market, they pose issues of limited use temperature and mechanical strength. In contrast, bead foams prepared from engineering plastics exhibit superior temperature resistance and mechanical strength, which have received much attention in recent years. Various engineering polymers, including poly (ether imide) (PEI) [22,73], polyimide (PI) [74], polyamide (PA) [75,76], polybutylene terephthalate (PBT) [19,77] and polycarbonate (PC) [78,79], have been employed in producing bead foams.

3. Molding of bead foams

The individual foamed beads typically need to be molded into three-dimensional parts through a molding process. The key to the molding stage is to keep the integrity of the cell structure and

 doi:10.20944/preprints202309.0439.v1

ensure sufficient inter-bead bonding strength. Bead foams in the molded parts must have sufficient welding strength to prevent the beads from falling off during use. According to the different welding mechanism of bead foams, it can be divided into steam-chest molding (SCM), adhesive-assisted molding (AAM), in-mold foaming and molding (IMFM) and microwave selective sintering (MSS).

3.1. Steam-chest molding (SCM)

Steam-chest molding (SCM) is an important bead foam molding technology, which was first used to produce EPS parts, and has the advantages of high production efficiency and the ability to produce large-sized products [4,16,72,80]. The wide adjustable temperature range and high latent heat make saturated steam capable of rapid heating. High pressure saturated steam is used as a heat transfer medium to heat the foamed beads in SCM, so that the beads are softened, and the interfacial diffusion and entanglement of molecular chains between the beads are realized under huge compression force. Single bead foams become molded parts with complex geometry after SCM.

The main equipment involved in SCM includes a steam generator, a feed system, and a SCM machine. The molding process of the bead foams is realized in the SCM machine. The description of SCM could be found in literature [71,81]. As depicted in Figure 9, the whole molding cycle can be divided into several steps.

Ⅰ. The movable mold is shifted to close the mold. At this stage, a certain gap is maintained according to the final thickness of the products. The foamed beads are injected into the mold to fill the cavity, and then the mold is closed to the final position.

Ⅱ. The high-pressure saturated steam enters the mold cavity through the gas nozzles and heats the foamed beads. In order to obtain a uniform temperature profile, the steam is usually introduced in the following order: double-sided preheating, cross- steam from the fixed mold and then from the movable mold, simultaneous steaming from the double molds (Figure 9 c-e). Steam pressure and steaming time are the key parameters during the process. In the heating step, the formation of inter-bead bonding between adjacent beads determines the mechanical properties of the final parts.

Ⅲ. Cool water is sprayed onto the mold surface to cool the mold and the molded parts. Cooling can freeze the molecular chains that diffuse and entangle in the welded interface and eliminate the adverse effect of high temperature on the cell structure and the dimensional stability of the product [82]. Compressed air is then used to blow off the condensation water, and most of the remaining water is removed by vacuum.

Ⅳ. In the final step, the molds open and the molded part is ejected.

In addition to conventional EPS [8] and EPP [10,11,13,42,83], SCM can be used to mold ETPU [4,16] and EPLA [72] parts and even to produce engineering plastic molded parts such as EPC and expanded polybutylene terephthalate (EPBT) parts [78,80]. As an amorphous polymer, the T_g of PS is around 100 °C and the temperature of saturated steam used to mold EPS beads is 107 – 120 °C. The molding temperature of EPP beads is usually in the range of 120 – 150 °C, which is dependent on the molecular chain structure and expansion ratio of EPP foamed beads [11,13,42,84]. Zhai et al. molded ETPU beads with different bead densities (e.g., 0.24, 0.29, and 0.35 g/cm^3) and investigated the molding behavior of the beads and mechanical performance of ETPU parts. The molding temperature was 135.7 °C. They found that all the beads had good inter-bead bonding and the tensile strength of the molded part was increased from 0.91 MPa to 1.80 MPa. Accompanying this increase in tensile strength was an increase in the elongation at break of the parts from 163.1% to 360.1%. Additionally, ETPU parts showed excellent deformation recovery ability. The ETPU cell structure remained stable after 200 compression cycle at 60% strain. In a more recent study, Jiang et al. prepared EPEBA parts using two types of foamed beads with different hardness [55]. EPEBA parts had a low density of less than 0.15 g/cm^3 and a high resilience above 70%.

Many research studies have been conducted by Altstädt et al. to prepare bead foam parts based on engineering materials [19,76,78,80,85,86]. They produced EPBT beads by extrusion foaming equipped with an underwater granulator [85]. It was found that EPBT beads with finer cell morphology and lower density could be obtained by incorporating a chain extender. An SCM machine with a customized steam generator was used to weld the foamed beads. The steam

Preprints (www.preprints.org) | NOT PEER-REVIEWED | Posted: 7 September 2023 doi:10.20944/preprints202309.0439.v1

temperature was in the range of 192 – 205 °C. It was found that the pure EPBT beads could not be molded; however, the chemically modified EPBT beads could be welded into final parts. EPBT parts showed a lowest density of 167 kg/m^3 and excellent thermal stability under compression. Using similar processing techniques, they also prepared expanded polyamide 12 bead foams [76] and expanded polycarbonate [78].

SCM has been utilized for over 70 years, and how to reduce the energy consumption of the molding process, how to improve the molding efficiency, and how to improve the welding strength of the bead foams are common concerns in both academia and industry. Aiming to reduce the temperature variation among the beads during molding process, Hossieny et al. [87] introduced hot air as a second heat transfer medium in the steam line. Since the hot air has a low Joule–Thompson coefficient, using a of mixture heating media could improve the surface quality and enhance the tensile strength of the molded EPP parts. As a result, the steaming time was reduced by approximately 32% and the molding temperature decreased by 16 °C. The results reveal that the incorporation of a certain amount of hot air in combination with saturated steam during the molding process can increase molding efficiency and reduce energy consumption.

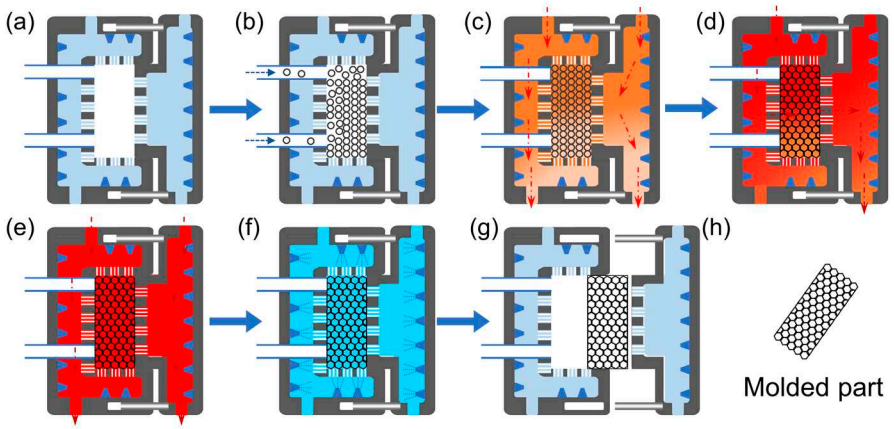

Figure 9. The molding steps of a complete SCM process.

3.2. Adhesive-assisted molding (AAM)

Adhesive-assisted molding (AAM) is a process that involves coating foamed beads with a particular adhesive, filling the coated beads into a mold, and finally solidifying the adhesive to produce bead foam parts. The use of AAM is possible with all types of foamed beads provided the appropriate adhesive and curing process selection. Welding foamed beads in a traditional SCM machine is a challenging task, especially for engineering plastics with high T_m or T_g. Nonetheless, AAM has been demonstrated as a viable method to produce molded parts using foamed beads made of engineering plastic. Zhai et al. [74] firstly fabricated lightweight expanded polyimide (EPI) parts with the assistance of AAM. EPI beads were prepared using solid-state foaming technique, where CO_2 and tetrahydrofuran were utilized as the main and co-blowing agents, respectively. The molding process used a PEI/chloroform solution as the adhesive. First, the solution-coated EPI beads were transferred to a mold, and then the adhesive layers among beads were solidified by heating and compression. EPI parts had the lowest density of 115.5 kg/m^3 and a flexural strength of 0.51 MPa. In another study related to AAM, Jiang et al. [22] prepared expanded poly(ether imide) (EPEI) parts using epoxy resin as the inter-bead bonding material. EPEI bead foams with an expansion ratio of 30–56 times were obtained by temperature rising foaming with CO_2/acetone as the mixed foaming agent. As illustrated in Figure 10, EPEI beads were coated with epoxy resin and then filled into a mold cavity, and finally the bonding layers were cured by heat compression to produce molded EPEI products. EPEI parts had a low density of 80 – 200 kg/m^3, high thermal stability at 160 °C and superior flame-retardant abilities. In recent work [23,24], flexible EPEBA parts have been fabricated by AAM.

Preprints (www.preprints.org) | NOT PEER-REVIEWED | Posted: 7 September 2023 doi:10.20944/preprints202309.0439.v1

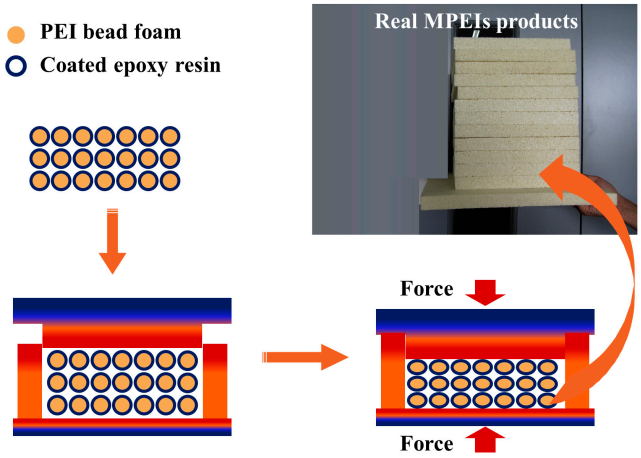

Figure 10. Schematic illustration of the compression molding process of the EPEI beads and MPEI specimens. Reproduced with permission from [22]. Copyright 2020 American Chemical Society.

AAM can be easily scaled up to industrial scale. Molded parts with complex geometry and large size can be produced by AAM. Especially for bead foams that cannot not be welded by conventional SCM, AAM provides another feasible approach.

3.3. In-mold foaming and molding (IMFM)

Recently, some attempts have been made to prepare bead foam parts by synergizing the constrained expansion of foamed beads with simultaneous welding under high temperature conditions [6,25,88-90]. Figure 11 shows the schematic of such in-mold foaming and molding (IMFM) process. Typically, the polymer pellets expand freely upon depressurization and the solid beads become foamed beads or bead foams. If the potential expansion volume of the foamed beads is greater than the mold cavity, the expanded beads will deform at the contacts with adjacent beads, creating an enormous compression force between neighboring beads. High temperature and high contact pressure allow the interdiffusion of polymer chains at the interface between the expanded beads. Meanwhile, the high pressure gas inside the cells maintains the stability of the cell structure. After a certain welding time, the mold is cooled in cool water, then the mold is opened, and bead foam parts are produced.

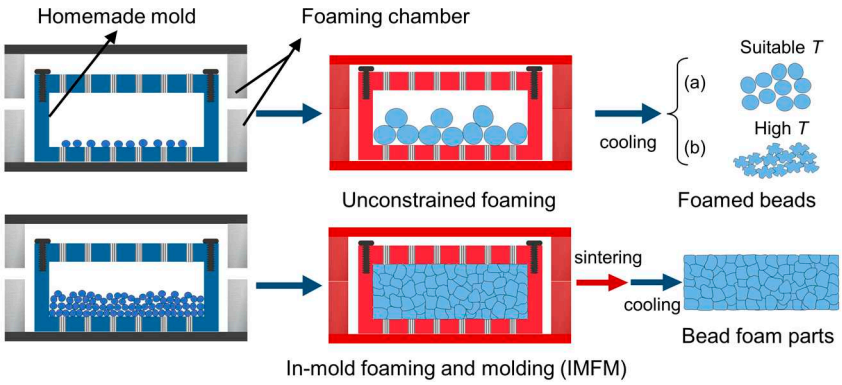

Figure 11. Schematic of unstrained foaming and in mold foaming and molding (IMFM) process. Reproduced with permission from [25]. Copyright 2023 Elsevier.

In this method, increasing the foaming temperature enhances the molecular mobility and increases the compression ratio of the expanded beads, both of which contribute to improving the inter-bead bonding strength. As shown in Figure 12 A, the ETPU parts exhibited clear inter-bead interfaces. An increase in foaming temperature from 144 °C to 150 °C resulted in the increase of cell size from 29 μm to 42 μm and reduction of cell wall thickness from 2.65 μm to 1.28 μm. ETPU parts

Preprints (www.preprints.org) | NOT PEER-REVIEWED | Posted: 7 September 2023 doi:10.20944/preprints202309.0439.v1

obtained at higher temperature showed improved welding strength. The elongation at break and tensile strength both increased with rising temperature (Figure 12 B). Meanwhile, the failure pattern of the molded parts changed from intra-bead fracture to inter-bead fracture. The good inter-bead bonding strength demonstrated that using IMFM is a feasible way to produce bead foam parts without the need for additional molding processes.

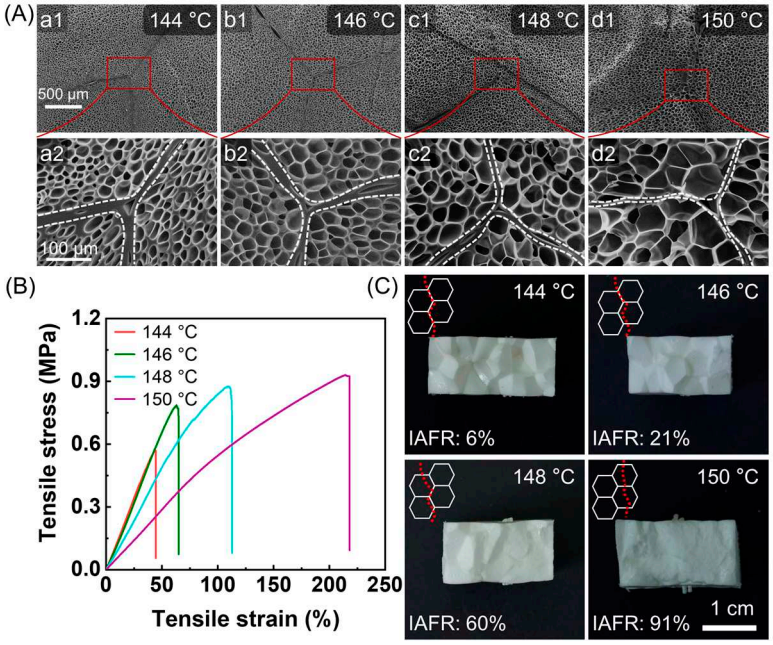

Figure 12. The microcellular structure of the cross-section of ETPU parts (A), tensile stress-strain curves of ETPU parts (B), fracture surface of ETPU parts after tensile test. The loading weight was 23 g, and the sintering time was 120 s. Reproduced with permission from [25]. Copyright 2023 Elsevier.

This strategy has been used to fabricate bead foam parts using various polymers like PEI [89], polyphenylene oxide/high-impact polystyrene composite [6] and poly(butylene adipate-co-terephthalate) blend [88]. IMFM is a simple and efficient method for bead foam part fabrication; however, it remains challenging to prepare products of large size with complex geometry.

3.4. Microwave selective sintering (MSS)

Microwaves belong to a type of special electromagnetic waves with frequencies ranging from 300 MHz to 300 GHz [91]. Microwave radiation can induce violent molecular vibrations and collisions, resulting in the release of large amounts of heat. In polymer processing, microwave heating can be used to weld different polymer parts (called microwave welding) [92]. Most plastics are "transparent" to microwaves, so microwave absorbers such as carbon nanotubes and carbon black are often used in microwave welding. Figure 13 shows the fabrication process of bead foam parts using microwave selective sintering (MSS). First, expanded/expandable beads are coated with conductive materials by ball milling. Second, the coated beads are filled into a poly(tetrafluoroethylene) (PTFE) mold. Third, the PTFE mold is placed in a microwave oven for molding. Rapid heating induced by microwave irradiation occurs at the interface between the beads. Finally, after sufficient cooling, the mold is opened, and the bead foam parts are obtained. During the molding process, loading weight, the power and sintering time are the key parameters. These parameters should be optimized to prepare final parts with good weld strength and surface quality.

Preprints (www.preprints.org) | NOT PEER-REVIEWED | Posted: 7 September 2023 doi:10.20944/preprints202309.0439.v1

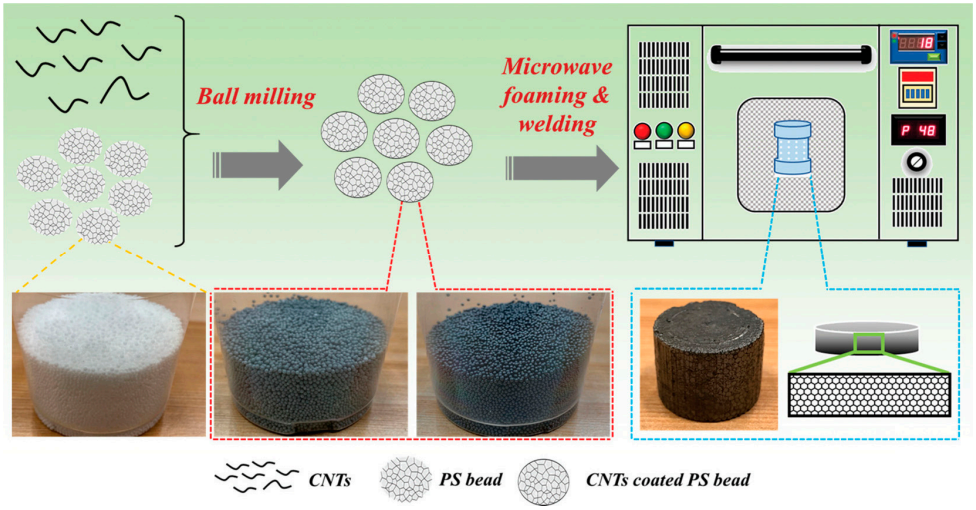

Figure 13. Schematic showing the microwave-assisted foaming and sintering to prepare EPEI parts. Reproduced with permission from [73]. Copyright 2020 American Chemical Society.

Using carbon nanotubes [73,93,94] or graphene nanoplatelets [95] as the conductive materials, Feng et al. have done much work on fabrication EPEI parts using MSS. MSS has also been used to prepare bead foam parts from PS [27,96] and PVA [97]. Using water as the dielectric material, Liu et al. [27] fabricated EPS parts with enhanced weld strength. The tensile strength of the molded parts was 2.3 MPa, two times higher than that of the counterpart prepared by conventional SCM. Selective and rapid heating characteristics make MSS a promising alternative to bead foam parts fabrication.

Table 1 compares the characteristics of various preparation methods. Although AAM, IMFM, and MSS have their unique advantages over SCM, they are mainly dominated by laboratory research. Despite its limitations in moldable materials, SCM remains the optimal choice for the large-scale production of bead foam parts.

Table 1. The characteristics of different molding method.

Process	Number of steps	Weld strength	Product size	Product density	Suitable material
SCM	two	high	large	Very low	limited
AAM	two	very high	large	low	wide
IMFM	one	high	small	low	wide
MSS	two	very high	small	low	wide

4. Mechanism of inter-bead bonding

For bead foams fabrication, the inter-bead bonding mechanism is the crucial problem. Only bead foam parts with enough bonding strength are useful in practical applications. Hence, the molding mechanism of bead foams has long been a subject of interest for researchers. Cross-section of the molded parts produced by various molding processes are compared in Figure 14. The figure highlights that the final products produced by diverse molding processes has different inter-bead interfaces, which is linked to the heat transfer process during molding. In this section, the inter-bead bonding mechanism of different molding processes will be discussed.

Preprints (www.preprints.org) | NOT PEER-REVIEWED | Posted: 7 September 2023 doi:10.20944/preprints202309.0439.v1

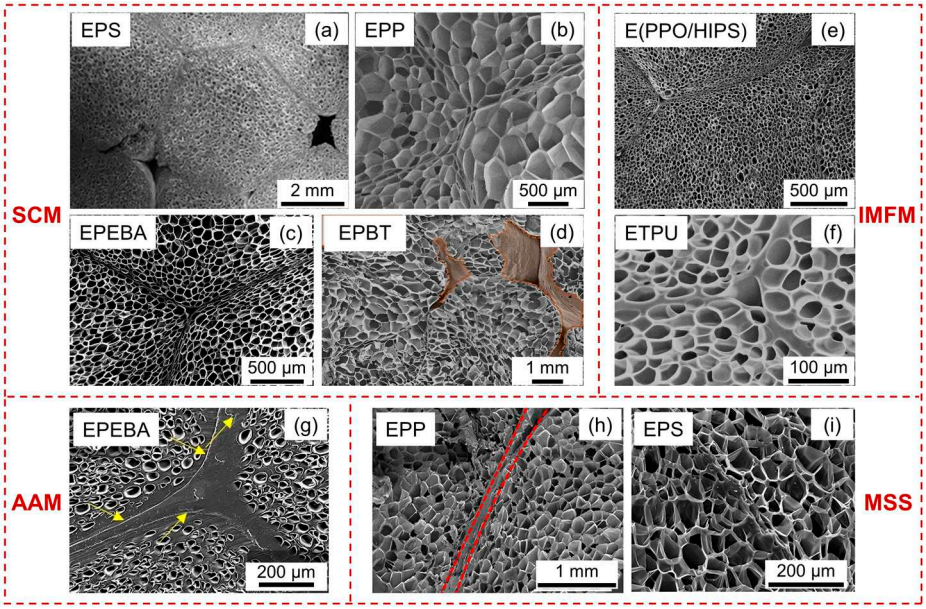

Figure 14. Cross-section of various bead foams parts prepared by different molding process. EPS parts (a), reproduced with permission from [33]. Copyright 2017 Taylor & Francis. EPP parts (b), reproduced with permission from [13]. Copyright 2022 American Chemical Society. EPEBA parts (c), reproduced with permission from [55]. Copyright 2022 Elsevier. EPBT parts (d), reproduced with permission from [98]. E(PPO/HIPS), expanded polyphenylene oxide/high-impact polystyrene composite (e), reproduced with permission from [6]. Copyright 2021 Wiley-VCH GmbH. ETPU parts (f), reproduced with permission from [25]. Copyright 2023 Elsevier. EPEBA parts (g), reproduced with permission from [24]. Copyright 2021 Elsevier. EPP parts (h), reproduced with permission from [26]. Copyright 2022 Elsevier. EPS parts (i), reproduced with permission from [27]. Copyright 2021 American Chemical Society.

For SCM process, as depicted in Figure 15, saturated steam undergoes a phase change on the surface of the foamed beads, releasing a substantial amount of latent heat. As a result, the foamed beads can be heated up rapidly and expand to a certain extent. In the case of EPS beads, the pentane inside the cell vaporizes during molding, leading to a second expansion of the foamed beads. In the case of ETPU and EPP, the beads are impregnated with low-pressure air before molding, and the bead foams can also expand when subjected to heat during the molding process. In the mold, the expanded bead foams are compressed into each other and transformed from ellipsoid to polyhedron, resulting in a significant increase in the contact area of adjacent beads. Polymer welding theory suggests that increasing the contact area and applied pressure can facilitate the diffusion of molecular chains [99,100]. As the heat accumulates at the interface, it causes a slight melting of the surface of the beads, which leads to interdiffusion across the interface and thereby resulting in the bonding between the foamed beads. As shown in Figure 14 a–d, high temperature and compression result in the contraction of cells near the interface region, thereby decreasing the uniformity of the cells in the molded parts. Furthermore, due to the low thermal conductivity of the cellular structure, the heating rate decreases radially along the skin layer toward the core layer of the foamed beads (Figure 15). Jiang et al. found a dependence of the polymer's softening point (T_s) on the heating rate, as higher heating rates result in lower T_s. Variations in T_s provide indirect evidence that explains the bonding behavior of ETPU and EPEBA beads during SCM.

Preprints (www.preprints.org) | NOT PEER-REVIEWED | Posted: 7 September 2023 doi:10.20944/preprints202309.0439.v1

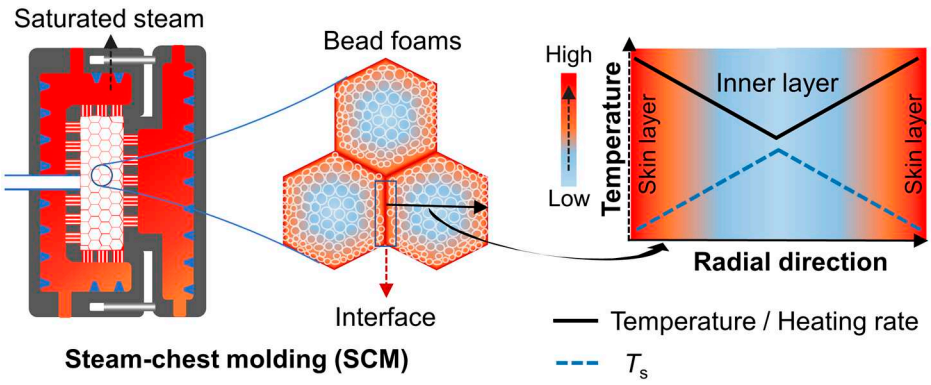

Figure 15. Schematic of the heat transfer process in SCM process. Reproduced with permission from [55]. Copyright 2022 Elsevier.

In addition to the heat transfer behavior of steam in foamed beads, the properties of polymers are the main factor responsible for the bonding of foamed beads. PS has a T_g of approximately 100 °C, the saturated steam used to mold EPS beads is 107 – 120 °C. During molding, EPS beads soften in the mold cavity due to steam heating, causing expansion of the pentane inside the cells and bringing close contact between the beads. At the interface, the molecular chains from adjacent beads initially form van der Waals interactions and then diffuse and entangle under the compression to achieve inter-bead bonding of EPS beads. TPU has a low crystallinity, and the ETPU beads exhibit a widely distributed hard domains and display a wide endothermic peak. During molding, the rapid heating of steam lowers the T_s of the skin layer of bead foam, causing the low-order hard segment phase to melt and promoting the interdiffusion of soft segments. This, in turn, promotes the movement of hard domains chains at the interface. During the cooling stage, the molecular chains that diffuse at the interface solidify to form a new hard segment domain with low order. The full diffusion and entanglement of the soft segment chains and rearrangement of the ordered hard segment domains endow ETPU parts with good inter-bead bonding strength. Numerous studies have studied the preparation and molding mechanism of EPP beads. By utilizing DSC to simulate the thermal behavior of EPP beads during SCM, along with analyzing the thermal behavior and mechanical properties of EPP parts fabricated by different temperature steam, Zhai et al. proposed a molding mechanism for EPP beads. EPP beads exhibit double melting peaks. The higher melting point ($T_{m\text{-}high}$) corresponds to the more close-packed and thick crystal area formed during the saturation process in autoclave. The lower melting point ($T_{m\text{-}low}$) corresponds to the less complete crystals formed during the cooling stage after foaming. At the steam temperature, the crystals on the surface of bead foams related to $T_{m\text{-}low}$ melt, significantly enhancing the molecular mobility at the interface. Additionally, the crystalline region corresponding to $T_{m\text{-}high}$ remains stable, supporting the stability of the cell structure. Under steam heating, the partial melted molecular chains diffuse and entangle at the interface between neighboring beads. Following rapid water cooling, the entangled chains recrystallize and freeze, creating a welding area at the inter-bead interfaces. In the study on SCM of EPBT beads, Ruckdäschel et al. [19] found that molecular weight plays a key factor in the moldability of bead foams. EPBT beads with a lower molecular weight exhibit higher porosity, compromising the stability of the bead foams during steam heating, and resulting in inability to bond the beads. Foamed beads prepared using higher molecular weight resin have a lower open cell content, allowing inter-bead bonding via SCM. When the molecular weight becomes too large, the molecular mobility is limited, leading to a decrease in the bonding strength of the bead foams.

In IMFM, due to the limited mold cavity, the expansion of the foaming beads is seriously restricted, which causes huge compression forces between the beads. As illustrated in Figure 16, constrained expansion results in smaller cell sizes and thicker bubble walls when compared to free foaming. The high-pressure gas within the cells remains the stability of the expanded beads. The high temperature environment and immense compressive stress facilitate interface welding. Under a certain sintering time, the chains interdiffusion and entanglement at inter-bead interface is realized and the beads are welded. As shown in Figure 16 d, IMFM requires the selection of appropriate

Preprints (www.preprints.org) | NOT PEER-REVIEWED | Posted: 7 September 2023 doi:10.20944/preprints202309.0439.v1

foaming conditions, and the combination of space constraint and sintering time to achieve sufficient inter-bead bonding.

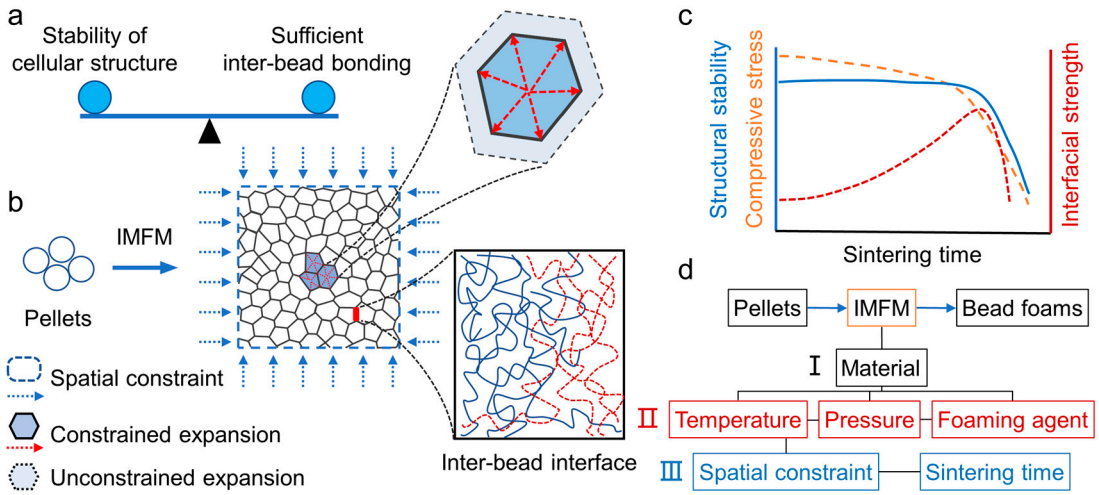

Figure 16. The mechanism of the restricted expansion and in-situ inter-bead bonding in IMFM process. Reproduced with permission from [25]. Copyright 2023 Elsevier.

For AAM, the key factor is selecting the suitable adhesive and curing process to ensure the stability of the bead foams. There are no demands on the porosity of the foamed beads. The molded parts prepared by AAM is characterized by a clear cured layer at the interface, as shown in Figure 14 g.

MSS has utilized the selective heating of microwave absorbents to weld bead foams together with microwave technology. As shown in Figure 14 h, a layer of microwave absorbents is clearly present between the expanded beads. Upon exposure to microwave radiation, a significant amount of heat is generated at the interface, which leads to interfacial welding between adjacent beads. When water is used as the medium for microwave absorption, the boundary becomes between the beads becomes less distinct (Figure 14 i). Like other molding processes, it is necessary to form an adequate contact area between the beads for inter-bead bonding. To achieve, it is vital to add enough bead foams to the mold prior to molding.

5. Conclusion and future perspectives

Bead foam constitutes a substantial portion of plastic foams prepared by physical foaming and its market share is on the rise. This review article has comprehensively examined the production methods of foamed beads, various molding techniques, and the inter-bead bonding mechanism during molding. While traditional bead foam remains prominent, attention has recently shifted towards foamed beads crafted from engineering plastics. This dynamic shift has led to the development of innovative molding techniques that sidestep the use of water vapor, effectively surmounting the temperature constraints inherent in conventional water vapor molding. Among the various molding processes, the mechanisms behind AAM and MSS stand out for their simplicity and clarity. Conversely, SCM and IMFM hinge significantly on factors such as the polymer's chemical composition, condensed structure, and stress for ensuring the successful bonding of foamed beads.

The intricate architecture of bead foam products coupled with the array of polymer choices have facilitated the creation of bead foam products with a spectrum of distinctive properties. While engineering plastics bead foam products have received much attention, the realization of a mature product line based on engineering plastics remains a challenge. This challenge is two-fold: first, achieving efficient preparation of engineering plastic foam beads with low open cell content and high expansion ratio; and second, tackling the complexities involved in molding these specialized bead foams.

The trajectory for future advancements in bead foaming technology encompasses recycling strategies for bead foam products, reduction of energy consumption in the manufacturing process, and the development of biodegradable bead foam. Evidently, bead foams have garnered escalating attention as a substantial and noteworthy category within the broader domain of foam products.

Author Contributions: Conceptualization, Junjie Jiang and Wentao Zhai; data curation, Liang Wang, Fangwei Tian and Yaozong Li; writing—original draft preparation, Junjie Jiang; writing—review and editing, Junjie Jiang and Wentao Zhai; visualization, Liang Wang, Fangwei Tian and Yaozong Li; supervision, Wentao Zhai; funding acquisition, Wentao Zhai. All authors have read and agreed to the published version of the manuscript.

Funding: Please add: This research was financially supported by the National Natural Science Foundation of China (52173053).

Data Availability Statement: The data are fully included in the article.

Acknowledgments: The authors are grateful to the National Natural Science Foundation of China (52173053).

Conflicts of Interest: The authors declare no conflict of interest.

References

1. Zhai, W. T.; Jiang, J. J.; Park, C. B., A review on physical foaming of thermoplastic and vulcanized elastomers. *Polym. Rev.* **2021,** *62*, 95-141.
2. Wu, G. J.; Xie, P. C.; Yang, H. G.; Dang, K. F.; Xu, Y. X.; Sain, M.; Turng, L. S.; Yang, W. M., A review of thermoplastic polymer foams for functional applications. *J. Mater. Sci.* **2021**, *56*, 11579-11604.
3. Jiang, J. J.; Zheng, H.; Liu, H. W.; Zhai, W. T., Tunable cell structure and mechanism in porous thermoplastic polyurethane micro-film fabricated by a diffusion-restricted physical foaming process. *J. Supercrit. Fluids* **2021**, *171*, 105205.
4. Jiang, J. J.; Liu, F.; Yang, X.; Xiong, Z. J.; Liu, H. W.; Xu, D. H.; Zhai, W. T., Evolution of ordered structure of TPU in high-elastic state and their influences on the autoclave foaming of TPU and inter-bead bonding of expanded TPU beads. *Polymer* **2021**, *228*, 123872.
5. Kuhnigk, J.; Standau, T.; Dörr, D.; Brütting, C.; Altstädt, V.; Ruckdäschel, H., Progress in the development of bead foams – A review. *J. Cell. Plast.* **2022**, *58*, 1-29.
6. Jiang, J. J.; Tian, F. W.; Zhou, M. N.; Li, M. Y.; Xiong, Z. J.; Gao, N.; Liu, H. W.; Zhai, W. T., Fabrication of lightweight polyphenylene oxide/high-impact polystyrene composite bead foam parts via in-mold foaming and molding technology. *Adv. Eng. Mater*. **2021**, *24*, 2101100.
7. Yan, J.; Wu, H.; Huang, P.; Wang, Y.; Shu, B.; Li, X.; Ding, D.; Sun, Y.; Wang, C.; Wu, J.; Sun, L., Investigation on the controllable synthesis of colorized and magnetic polystyrene beads with millimeter size via in situ suspension polymerization. F*rontiers in Chemistry* **2022**, *10*, 891582.
8. Prasittisopin, L.; Termkhajornkit, P.; Kim, Y. H., Review of concrete with expanded polystyrene (EPS): Performance and environmental aspects. *J. Cleaner Prod.* **2022**, *366*, 132919.
9. Guo, P.; Xu, Y.; Lu, M.; Zhang, S., expanded linear low-density polyethylene beads: fabrication, melt strength, and foam morphology. *Ind. Eng. Chem. Res.* **2016**, *55*, 8104-8113.
10. Tammaro, D.; Ballesteros, A.; Walker, C.; Reichelt, N.; Trommsdorff, U., Expanded beads of high melt strength polypropylene moldable at low steam pressure by foam extrusion. *Polymers*, **2022**, *14*, 205.
11. Su, Y.; Huang, P.; Luo, H.; Chong, Y.; Zhao, Y.; Wu, M.; Zheng, H.; Lan, X.; Wu, F.; Zheng, W., Supercritical CO_2 extrusion foaming and steam-chest molding of polypropylene/thermoplastic polyurethane bead foams. *ACS Appl. Polym. Mater.* **2022**, *4*, 9441-9448.
12. Huang, P. K.; Su, Y. Z.; Luo, H. B.; Lan, X. Q.; Chong, Y. K.; Wu, F.; Zheng, W. G., Facile one-step method to manufacture polypropylene bead foams with outstanding thermal insulation and mechanical properties via supercritical CO_2 extrusion foaming. *J. CO2 Util.* **2022**, *64*, 102167.
13. Guo, P.; Xu, Y.; Lyu, M.; Zhang, S., Fabrication of expanded ethylene–propylene–butene-1 copolymer bead. *Ind. Eng. Chem. Res.* **2022**, *61*, 2392-2402.
14. Zhang, T.; Lee, S.-J.; Yoo, Y. H.; Park, K.-H.; Kang, H.-J., Compression molding of thermoplastic polyurethane foam sheets with beads expanded by supercritical CO_2 foaming. *Polymers* **2021**, *13*, 656.
15. 15. Singaravelu, A. S. S.; Williams, J. J.; Ruppert, J.; Henderson, M.; Holmes, C.; Chawla, N., In situ X-ray microtomography of the compression behaviour of eTPU bead foams with a unique graded structure. *J. Mater. Sci.* **2021**, *56*, 5082-5099.
16. Ge, C. B.; Ren, Q.; Wang, S. P.; Zheng, W. G.; Zhai, W. T.; Park, C. B., Steam-chest molding of expanded thermoplastic polyurethane bead foams and their mechanical properties. *Chem. Eng. Sci.* **2017**, *174*, 337-346.

17. Su, Y.; Huang, P.; Sun, J.; Chen, J.; Zheng, H.; Luo, H.; Chong, Y.; Zhao, Y.; Wu, F.; Zheng, W., Extruded polylactide bead foams using anhydrous supercritical CO_2 extrusion foaming. *J. Appl. Polym. Sci.* **2023**, *n/a*, e54557.
18. Chauvet, M.; Sauceau, M.; Fages, J., Extrusion assisted by supercritical CO_2: A review on its application to biopolymers. *J. Supercrit. Fluids* **2017**, *120*, 408-420.
19. Kuhnigk, J.; Krebs, N.; Mielke, C.; Standau, T.; Pospiech, D.; Ruckdäschel, H., Influence of molecular weight on the bead foaming and bead fusion behavior of poly(butylene terephthalate) (PBT). *Ind. Eng. Chem. Res.* **2022**, *61*, 17904-17914.
20. 20. Shabani, A.; Fathi, A.; Erlwein, S.; Altstädt, V., Thermoplastic polyurethane foams: from autoclave batch foaming to bead foam extrusion. *J. Cell. Plast.* **2021**, *57*, 391-411.
21. Singaravelu, A. S. S.; Williams, J. J.; Shevchenko, P.; Ruppert, J.; De Carlo, F.; Henderson, M.; Holmes, C.; Chawla, N., Poisson's ratio of eTPU molded bead foams in compression via in situ synchrotron X-ray microtomography. *J. Mater. Sci.* **2021**, *56*, 12920-12935.
22. Jiang, J. J.; Feng, W. W.; Zhao, D.; Zhai, W. T., Poly(ether imide)/epoxy foam composites with a microcellular structure and ultralow density: Bead foam fabrication, compression molding, mechanical properties, thermal stability, and flame-retardant properties. *ACS Omega* **2020**, *5*, 25784-25797.
23. Ma, Z. L.; Wei, A. J.; Li, Y. T.; Shao, L.; Zhang, H. M.; Xiang, X. L.; Wang, J. P.; Ren, Q. B.; Kang, S. L.; Dong, D. D.; Ma, J. O.; Zhang, G. C., Lightweight, flexible and highly sensitive segregated microcellular nanocomposite piezoresistive sensors for human motion detection. *Compos. Sci. Technol.* **2021**, *203*, 108571.
24. Ge, C.; Wang, G.; Zhao, G.; Wei, C.; Li, X., Lightweight and flexible poly(ether-block-amide)/multiwalled carbon nanotube composites with porous structure and segregated conductive networks for electromagnetic shielding applications. *Compos. Part A* **2021**, *144*, 106356.
25. Jiang, J.; Chen, B.; Zhou, M.; Liu, H.; Li, Y.; Tian, F.; Wang, Z.; Wang, L.; Zhai, W., A convenient and efficient path to bead foam parts: Restricted cell growth and simultaneous inter-bead welding. *J. Supercrit. Fluids* **2023**, *194*, 105852.
26. Ding, M.; Xu, D.; Wang, Q., Microwave-assisted foaming and sintering high-strength and antistatic polypropylene bead foams by constructing conductive 3D skeleton structure. *Compos. Part A* **2022**, *163*, 107196.
27. Yang, J.; Chen, Z.; Xu, D.; Liu, P.; Li, L., Enhanced interfacial adhesion of polystyrene bead foams by microwave sintering for microplastics reduction. *Ind. Eng. Chem. Res.* **2021**, *60*, 8812-8820.
28. Dreier, J.; Brütting, C.; Ruckdäschel, H.; Altstädt, V.; Bonten, C., Investigation of the thermal and hydrolytic degradation of polylactide during autoclave foaming. *Polymers*, **2021**, *13*, 2624.
29. Sands, M.; Shivkumar, S., EPS bead fusion effects on fold defect formation in lost foam casting of aluminum alloys. *J. Mater. Sci.* **2006**, *41*, 2373-2379.
30. Doroudiani, S.; Omidian, H., Environmental, health and safety concerns of decorative mouldings made of expanded polystyrene in buildings. *Build.Environ.* **2010**, *45*, 647-654.
31. Yuan, B.; Wang, G.; Bai, S.; Liu, P., Preparation of halogen-free flame-retardant expandable polystyrene foam by suspension polymerization. *J. Appl. Polym. Sci.* **2019**, *136*, 47779.
32. Bhoite, S. P.; Kim, J.; Jo, W.; Bhoite, P. H.; Mali, S. S.; Park, K.-H.; Hong, C.-K., Expanded polystyrene beads coated with intumescent flame retardant material to achieve fire safety standards. *Polymers* **2021**, *13*, 2662.
33. Varnagiris, S.; Doneliene, J.; Tuckute, S.; Cesniene, J.; Lelis, M.; Milcius, D., Expanded polystyrene foam formed from polystyrene beads coated with a nanocrystalline SiO_2 film and the analysis of its moisture adsorption and resistance to mechanical stress. *Polymer. Plast. Technol. Eng.* **2018**, *57*, 1296-1302.
34. Jang, B. K.; Kim, M. H.; Park, O. O., Effects of crystallinity and molecular weight on the melting behavior and cell morphology of expanded polypropylene in bead foam manufacturing. *Macromol. Res.* **2020**, *28*, 343-350.
35. Weingart, N.; Raps, D.; Lu, M.; Endner, L.; Altstädt, V., Comparison of the foamability of linear and long-chain branched polypropylene—The legend of strain-hardening as a requirement for good foamability. *Polymers* **2020**, *12*, 725.
36. Guo, P.; Xu, Y.; Lu, M.; Zhang, S., High melt strength polypropylene with wide molecular weight distribution used as basic resin for expanded polypropylene beads. *Ind. Eng. Chem. Res.* **2015**, *54*, 217-225.
37. Guo, Y. T.; Hossieny, N.; Chu, R. K. M.; Park, C. B.; Zhou, N. Q., Critical processing parameters for foamed bead manufacturing in a lab-scale autoclave system. *Chem. Eng. J.* **2013**, *214*, 180-188.
38. 38. Nofar, M.; Guo, Y. T.; Park, C. B., Double crystal melting peak generation for expanded polypropylene bead foam manufacturing. *Ind. Eng. Chem. Res.* **2013**, *52*, 2297-2303.
39. Guo, P.; Liu, Y.; Xu, Y.; Lu, M.; Zhang, S.; Liu, T., Effects of saturation temperature/pressure on melting behavior and cell structure of expanded polypropylene bead. *J. Cell. Plast.* **2014**, *50*, 321-335.
40. Zhang, R.; Xiong, Y.; Liu, Q.; Hu, S., Improved cell morphology and thermal properties of expanded polypropylene beads by the addition of PP with a high melting point. *J. Appl. Polym. Sci.* **2017**, *134*, 45121.
41. Golmohammadi, M.; Salehabadi, M.; Janani, H., Role of polymorphism in solid-state production of double-melting expanded polypropylene beads. *Polymer* **2023**, *270*, 125757.

42. Lan, X.; Huang, P.; Chong, Y.; Wu, F.; Su, Y.; Luo, H.; Lee, P. C.; Zheng, W., Autoclave foaming and steam-chest molding of polypropylene/polybutene-1 blend bead foams and their crystallization and mechanical properties. *J. Cell. Plast.* **2023**, *59*, 29-45.
43. Lan, X. Q.; Zhai, W. T.; Zheng, W. G., Critical effects of polyethylene addition on the autoclave foaming behavior of polypropylene and the melting behavior of polypropylene foams blown with n-pentane and CO_2. *Ind. Eng. Chem. Res.* **2013**, *52*, 5655-5665.
44. Rizvi, A.; Chu, R. K. M.; Lee, J. H.; Park, C. B., Superhydrophobic and oleophilic open-cell foams from fibrillar blends of polypropylene and polytetrafluoroethylene. *ACS Appl. Mater. Interfaces* **2014**, *6*, 21131-21140.
45. Huang, P. K.; Wu, M. H.; Pang, Y. Y.; Shen, B.; Wu, F.; Lan, X. Q.; Luo, H.; Zheng, W. G., Ultrastrong, flexible and lightweight anisotropic polypropylene foams with superior flame retardancy. *Composites, Part A* **2019**, *116*, 180-186.
46. Huang, P.; Wu, F.; Shen, B.; Ma, X.; Zhao, Y.; Wu, M.; Wang, J.; Liu, Z.; Luo, H.; Zheng, W., Bio-inspired lightweight polypropylene foams with tunable hierarchical tubular porous structure and its application for oil-water separation. *Chem. Eng. J.* **2019**, *370*, 1322-1330.
47. Pang, Y. Y.; Wang, S. S.; Wu, M. H.; Liu, W.; Wu, F.; Lee, P. C.; Zheng, W. G., Kinetics study of oil sorption with open-cell polypropylene/polyolefin elastomer blend foams prepared via continuous extrusion foaming. *Polym. Adv. Technol.* **2018**, *29*, 1313-1321.
48. Tong, X.; Peng, W. M.; Zhang, M. L.; Wang, X. J.; Zhang, G.; Long, S. R.; Yang, J., A new class of poly(ether-block-amide)s based on semi-aromatic polyamide: synthesis, characterization and structure-property relations. *Polym. Int.* **2021**, *70*, 230-241.
49. Zhong, W. P.; Yu, Z.; Zhu, T. Y.; Zhao, Y. X.; Phule, A. D.; Zhang, Z. X., Influence of different ratio of CO_2/N_2 and foaming additives on supercritical foaming of expanded thermoplastic polyurethane. *Express Polym. Lett.* **2022**, *16*, 318-336.
50. Jiang, J. J.; Zhou, M. N.; Li, Y. Z.; Chen, B. C.; Tian, F. W.; Zhai, W. T., Cell structure and hardness evolutions of TPU foamed sheets with high hardness via a temperature rising foaming process. *J. Supercrit. Fluids* **2022**, *188*, 105654.
51. Chen, B.; Jiang, J.; Li, Y.; Zhou, M.; Wang, Z.; Wang, L.; Zhai, W., Supercritical fluid microcellular foaming of high-hardness TPU via a pressure-quenching process: restricted foam expansion controlled by matrix modulus and thermal degradation. *Molecules* **2022**, *27*, 8911.
52. Nofar, M.; Kucuk, E. B.; Bati, B., Effect of hard segment content on the microcellular foaming behavior of TPU using supercritical CO_2. *J. Supercrit. Fluids* **2019**, *153*, 104590.
53. Batı, B.; Küçük, E. B.; Durmuş, A.; Nofar, M., Microcellular foaming behavior of ether- and ester-based TPUs blown with supercritical CO_2. *J. Polym. Eng.* **2020**, *40*, 561-571.
54. Nofar, M.; Batı, B.; Küçük, E. B.; Jalali, A., Effect of soft segment molecular weight on the microcellular foaming behavior of tpu using supercritical CO_2. *J. Supercrit. Fluids* **2020**, *160*, 104816.
55. Jiang, J. J.; Liu, F.; Chen, B. C.; Li, Y. Z.; Yang, X.; Tian, F. W.; Xu, D. H.; Zhai, W. T., Microstructure development of PEBA and its impact on autoclave foaming behavior and inter-bead bonding of EPEBA beads. *Polymer* **2022**, *256*, 125244.
56. Hossieny, N.; Shaayegan, V.; Ameli, A.; Saniei, M.; Park, C. B., Characterization of hard-segment crystalline phase of thermoplastic polyurethane in the presence of butane and glycerol monosterate and its impact on mechanical property and microcellular morphology. *Polymer* **2017**, *112*, 208-218.
57. Barzegari, M. R.; Hossieny, N.; Jahani, D.; Park, C. B., Characterization of hard-segment crystalline phase of poly(ether-block-amide) (PEBAX®) thermoplastic elastomers in the presence of supercritical CO_2 and its impact on foams. *Polymer* **2017**, *114*, 15-27.
58. Hossieny, N. J.; Barzegari, M. R.; Nofar, M.; Mahmood, S. H.; Park, C. B., Crystallization of hard segment domains with the presence of butane for microcellular thermoplastic polyurethane foams. *Polymer* **2014**, *55*, 651-662.
59. Lu, J.; Zhang, H.; Chen, Y.; Ge, Y.; Liu, T., Effect of chain relaxation on the shrinkage behavior of TPEE foams fabricated with supercritical CO_2. *Polymer* **2022**, *256*, 125262.
60. Lan, B.; Li, P.; Yang, Q.; Gong, P., Dynamic self generation of hydrogen bonding and relaxation of polymer chain segment in stabilizing thermoplastic polyurethane microcellular foams. *Mater. Today Commun.* **2020**, *24*, 101056.
61. 61. Zhang, R.; Huang, K.; Hu, S. F.; Liu, Q. T.; Zhao, X. P.; Liu, Y., Improved Cell Morphology and Reduced Shrinkage Ratio of ETPU Beads by Reactive Blending. Polym. Test. 2017, 63, 38-46.
62. Ahmed, M. F.; Li, Y.; Yao, Z.; Cao, K.; Zeng, C. C., TPU/PLA blend foams: Enhanced foamability, structural stability, and implications for shape memory foams. *J. Appl. Polym. Sci.* **2019**, *136*, 47416-47427.
63. Zheng, H.; Huang, P.; Lee, P. C.; Chang, N. R. S.; Zhao, Y.; Su, Y.; Wu, F.; Liu, X.; Zheng, W., Lightweight olefin block copolymers foams with shrinkable and recoverable performance via supercritical CO_2 foaming. *J. Supercrit. Fluids* **2023**, *200*, 105981.

64. Zheng, H.; Pan, G.; Huang, P. K.; Xu, D. H.; Zhai, W. T., Fundamental influences of crosslinking structure on the cell morphology, creep property, thermal property, and recycling behavior of microcellular EPDM foams blown with compressed CO_2. *Ind. Eng. Chem. Res.* **2020**, *59*, 1534-1548.
65. Xu, Z.; Wang, G.; Zhao, J.; Zhang, A.; Dong, G.; Zhao, G., Anti-shrinkage, high-elastic, and strong thermoplastic polyester elastomer foams fabricated by microcellular foaming with CO_2 & N_2 as blowing agents. *J. CO2 Util.* **2022**, *62*, 102076.
66. Gao, X.; Chen, Y.; Chen, P.; Xu, Z.; Zhao, L.; Hu, D., Supercritical CO_2 foaming and shrinkage resistance of thermoplastic polyurethane/modified magnesium borate whisker composite. *J. CO2 Util.* **2022**, *57*, 101887.
67. Lan, B.; Li, P.; Luo, X.; Luo, H.; Yang, Q.; Gong, P., Hydrogen bonding and topological network effects on optimizing thermoplastic polyurethane/organic montmorillonite nanocomposite foam. *Polymer* **2021**, *212*, 123159.
68. Nofar, M.; Park, C. B., Poly (lactic acid) Foaming. *Prog. Polym. Sci.* **2014**, *39*, 1721-1741.
69. Nofar, M.; Ameli, A.; Park, C. B., Development of polylactide bead foams with double crystal melting peaks. *Polymer* **2015**, *69*, 83-94.
70. Standau, T.; Goettermann, S.; Weinmann, S.; Bonten, C.; Altstädt, V., Autoclave foaming of chemically modified polylactide. *J. Cell. Plast.* **2016**, *53*, 481-489.
71. Standau, T.; Zhao, C. J.; Castellon, S. M.; Bonten, C.; Altstaedt, V., Chemical modification and foam processing of polylactide (PLA). *Polymers* **2019**, *11*, 306.
72. Nofar, M.; Ameli, A.; Park, C. B., A novel technology to manufacture biodegradable polylactide bead foam products. *Mater. Des.* **2015**, *83*, 413-421.
73. Feng, D.; Liu, P.; Wang, Q., Selective microwave sintering to prepare multifunctional poly(ether imide) bead foams based on segregated carbon nanotube conductive network. *Ind. Eng. Chem. Res.* **2020**, *59*, 5838-5847.
74. Zhai, W. T.; Feng, W. W.; Ling, J. Q.; Zheng, W. G., Fabrication of lightweight microcellular polyimide foams with three-dimensional shape by CO_2 foaming and compression molding. *Ind. Eng. Chem. Res.* **2012**, *51*, 12827-12834.
75. Yeh, S.-K.; Liu, W.-H.; Huang, Y.-M., Carbon dioxide-blown expanded polyamide bead foams with bimodal cell structure. *Ind. Eng. Chem. Res.* **2019**, *58*, 2958-2969.
76. Dorr, D.; Raps, D.; Kirupanantham, D.; Holmes, C.; Altstadt, V., Expanded polyamide 12 bead foams (ePA) thermo-mechanical properties of molded parts. *AIP Conf. Proc.* **2020**, *2205*, 020037.
77. 77. Köppl, T.; Raps, D.; Altstädt, V., E-PBT—Bead foaming of poly(butylene terephthalate) by underwater pelletizing. *J. Cell. Plast.* **2014**, *50*, 475-487.
78. Weingart, N.; Raps, D.; Kuhnigk, J.; Klein, A.; Altstadt, V., Expanded polycarbonate (EPC) — A new generation of high-temperature engineering bead foams. *Polymers* **2020**, *12*, 2314.
79. Sánchez-Calderón, I.; Bernardo, V.; Martín-de-León, J.; Rodríguez-Pérez, M. Á., Novel approach based on autoclave bead foaming to produce expanded polycarbonate (EPC) bead foams with microcellular structure and controlled crystallinity. *Mater. Des.* **2021**, *212*, 110200.
80. Kuhnigk, J.; Raps, D.; Standau, T.; Luik, M.; Altstädt, V.; Ruckdäschel, H., Insights into the bead fusion mechanism of expanded polybutylene terephthalate (E-PBT). *Polymers* **2021**, *13*, 582.
81. Raps, D.; Hossieny, N.; Park, C. B.; Altstadt, V., Past and present developments in polymer bead foams and bead foaming technology. *Polymer* **2015**, *56*, 5-19.
82. Zhai, W. T.; Kim, Y. W.; Jung, D. W.; Park, C. B., Steam-chest molding of expanded polypropylene foams. 2. Mechanism of interbead bonding. *Ind. Eng. Chem. Res.* **2011**, *50*, 5523-5531.
83. Wu, F.; Li, Y.; Lan, X.; Huang, P.; Chong, Y.; Luo, H.; Shen, B.; Zheng, W., Large-scale fabrication of lightweight, tough polypropylene/carbon black composite foams as broadband microwave absorbers. *Compos. Commun.* **2020**, *20*, 100358.
84. Pin, J.-M.; Anstey, A.; Schubnell, M.; Lee, P. C., Two-dimensional correlation analysis of iPP bead foaming thermal features modeled by fast scanning calorimetry. *ACS Macro Letters* **2021**, *10*, 1280-1286.
85. Standau, T.; Hädelt, B.; Schreier, P.; Altstädt, V., Development of a bead foam from an engineering polymer with addition of chain extender: expanded polybutylene terephthalate. *Ind. Eng. Chem. Res.* **2018**, *57*, 17170-17176.
86. 86. Kuhnigk, J.; Krebs, N.; Standau, T.; Dippold, M.; Ruckdäschel, H., Evaluation of the fusion quality of bead foams made from polybutylene terephthalate (E-PBT) depending on the processing temperature. *Macromol. Mater. Eng.* **2022**, *307*, 2200419.
87. Hossieny, N.; Ameli, A.; Park, C. B., Characterization of expanded polypropylene bead foams with modified steam-chest molding. *Ind. Eng. Chem. Res.* **2013**, *52*, 8236-8247.
88. Cai, W.; Liu, P.; Bai, S.; Li, S., A one-step method to manufacture biodegradable poly (butylene adipate-co-terephthalate) bead foam parts. *Polym. Adv. Technol.* **2021**, *32*, 2007-2019.
89. Feng, D.; Li, L.; Wang, Q., Fabrication of three-dimensional polyetherimide bead foams via supercritical CO_2/ethanol co-foaming technology. *RSC Adv.* **2019**, *9*, 4072-4081.

90. Errichiello, F.; Cammarano, A.; Di Maio, E.; Nicolais, L., Sintering graded foamed beads: Compressive properties. *J. Appl. Polym. Sci.* **2022**, *139*, 52052.
91. Wang, C. Y.; Chen, T. H.; Chang, S. C.; Cheng, S. Y.; Chin, T. S., Strong Carbon–Nanotube–Polymer Bonding by Microwave Irradiation. *Adv. Funct. Mater.* **2007**, *17*, 1979-1983.
92. Sweeney, C. B.; Lackey, B. A.; Pospisil, M. J.; Achee, T. C.; Hicks, V. K.; Moran, A. G.; Teipel, B. R.; Saed, M. A.; Green, M. J., Welding of 3D-printed carbon nanotube-polymer composites by locally induced microwave heating. *Sci. Adv.* **2017**, *3*, e1700262.
93. Feng, D.; Wang, Q.; Xu, D.; Liu, P., Microwave assisted sinter molding of polyetherimide/carbon nanotubes composites with segregated structure for high-performance EMI shielding applications. *Compos. Sci. Technol.* **2019**, *182*, 107753.
94. Feng, D.; Liu, P. J.; Wang, Q., Carbon nanotubes in microwave-assisted foaming and sinter molding of high performance polyetherimide bead foam products. *Mater. Sci. Eng.*, B **2020**, *262*, 114727.
95. Feng, D.; Liu, P., Microwave-assisted rapid fabrication of robust polyetherimide bead foam parts. *J. Appl. Polym. Sci.* **2020**, *138*, 49960.
96. Xie, Y.; Li, Z.; Tang, J.; Li, P.; Chen, W.; Liu, P.; Li, L.; Zheng, Z., Microwave-assisted foaming and sintering to prepare lightweight high-strength polystyrene/carbon nanotube composite foams with an ultralow percolation threshold. *J. Mater. Chem. C* **2021**, *9*, 9702-9711.
97. Xu, D.; Liu, P.; Wang, Q., An ultrafast and clean method to manufacture poly(vinyl alcohol) bead foam products. *Polym. Adv. Technol.* **2021**, *32*, 210-219.
98. Standau, T.; Schreiers, P.; Hilgert, K.; Altstädt, V., Properties of bead foams with increased heat stability made from the engineering polymer polybutylene terephthalate (E-PBT). *AIP Conf. Proc.* **2020**, *2205*, 020039.
99. Bousmina, M.; Qiu, H.; Grmela, M.; Klemberg-Sapieha, J. E., Diffusion at polymer/polymer interfaces probed by rheological tools. *Macromolecules* **1998**, *31*, 8273-8280.
100. Wool, R. P.; Yuan, B. L.; McGarel, O. J., Welding of polymer interfaces. *Polym. Eng. Sci.* **1989**, *29*, 1340-1367.